Effect of Number of Elements of a Reactively-Loaded Ring Antenna Array on the Performance of Beamwidth Variation

Shinya Sugiura, *Member, IEEE,* Noriyoshi Suzuki, *Member, IEEE,* and Hideo Iizuka, *Member, IEEE*

***Abstract*— We herein investigate the effect of the number of elements of a previously studied reactively-loaded ring antenna array with respect to electronically variable beamwidth performance. The antenna has a unique ability to increase the effective antenna length by adding parasitic ring elements, which contributes to higher performance with respect to beamwidth variation. Monte Carlo (MC) simulations clarify that variable range of beamwidth can be improved effectively by increasing the number of ring elements M to five. It is herein demonstrated for the case of M = 5 that the beamwidth toward the broadside direction can be controlled from 40^o to 145^o in the E plane, while maintaining the voltage standing-wave ratio (VSWR) to less than 3.0, where the antenna size is 0.32$\lambda\times$1.32λ. In addition, it is also confirmed that the number of estimated directions-of-arrival (DOAs) based on the reactance-domain multiple signal classification (MUSIC) algorithm can be also increased by increasing the number of ring elements.**

***Index Terms*— Active antennas, antenna array, direction-of-arrival estimation, reactively steered antennas, parasitic elements, road vehicles, varactors, variable beamwidth.**

I. Introduction

VEHICLE-to-vehicle (V2V) communications have received a great deal of attention due to their potential for reducing the number of traffic accidents. The pattern-reconfigurable antenna is a promising choice for improving system performance [1]. While most of the previous studies have focused primarily on beam and/or null direction steering, beamwidth control is also expected to be effective for a simple algorithm based on terminal speed, i.e., broad beamwidth at low speed and narrow beamwidth at high speed, which does not require complicated cross-layer optimization.

A number of variable beamwidth antennas with a single RF branch have been developed. Most of these studies were based on the adjustment of geometrical parameters or on utilization of a phased array technique [2]-[5]. Lim *et al.* [6] were the first to propose an approach to tune beamwidth in an electronic manner, based on the composite right/left-handed (CRLH) leaky wave antenna technique, without changing the geometrical parameters.

The authors are with Toyota Central Research and Development Laboratories, Incorporated, Aichi 480-1192, Japan (e-mail: sugiura@mosk.tytlabs.co.jp; nori@mcl.tytlabs.co.jp; hiizuka@mosk.tytlabs.co.jp). S. Sugiura is also with the School of Electronics and Computer Science, University of Southampton, Southampton SO17 1BJ, U.K.

DOI: 10.1109/LAWP.2008.919815

In the field of single-feed pattern-reconfigurable antennas, reactively steered antennas have been developed extensively [7]-[9], focusing primarily on beam and/or null direction steering. There is difficulty in applying these antennas to beamwidth control, however, because the spacing between the feed element and the parasitic elements must be limited to less than approximately $\lambda/4$ in order for the feed element to maintain sufficient mutual couplings with parasitic elements. Thus, an effective antenna length that is of sufficient length for beamwidth control cannot be obtained in this configuration.

More recently, a conformal steerable antenna composed of three overlapping ring elements has been studied for automobile applications [10]. This antenna has the potential to increase the effective antenna length while maintaining strong mutual couplings. In the present paper, the beamwidth of the conformal steerable antenna is investigated with increasing the number of ring elements. Numerical investigations indicate that the beamwidth of the antenna is sufficiently narrow to use in beamwidth-variation application. The antenna configuration is presented in Section II. In addition, the formulation of the directivity is derived. In Section III, radiation patterns are calculated by Monte Carlo (MC) simulations, and the performance of the beamwidth variation is discussed. In addition, we mention another capability of high-resolution directions-of-arrival (DOAs) estimation based on the MUSIC algorithm, which can be expected to give additional information useful for improving beamwidth control as well as beam direction control. This paper is concluded in Section IV.

II. Antenna Configuration and Formulation

Fig. 1(a) and 1(b) show a top view and a side view of the proposed antenna configuration. This configuration is basically an extension of the configuration proposed in [10], where the number of ring elements was three. The proposed antenna is constructed of M one-wavelength ring elements, which are situated so as not to have any nodal point. The antenna has $2M$ ports, which are arranged along the y-axis. The kth port ($1 \leq k \leq 2M$) is chosen as a balanced feed point among the $2M$ ports, and variable reactance circuit are set at the remaining $2M-1$ ports. Both beamwidth and beam direction are controlled by changing the values of the circuits. The number of ring elements M and the antenna length W are related as $W = \lambda/\pi + (M-1)\,G$, where G represents the array spacing in the y direction. Note that $2M-1$ overlapping areas contribute to strong mutual couplings among

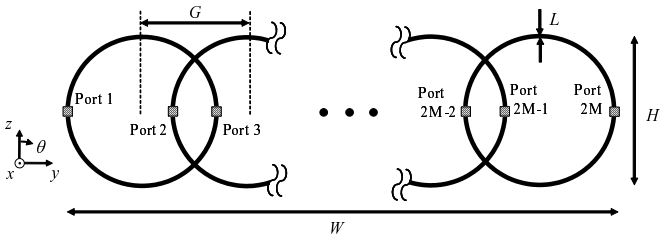

(a) Top view

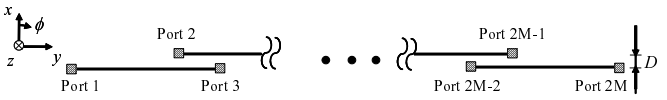

(b) Side view

Fig. 1. Configuration of the proposed antenna. Each figure shows (a) top view and (b) side view.

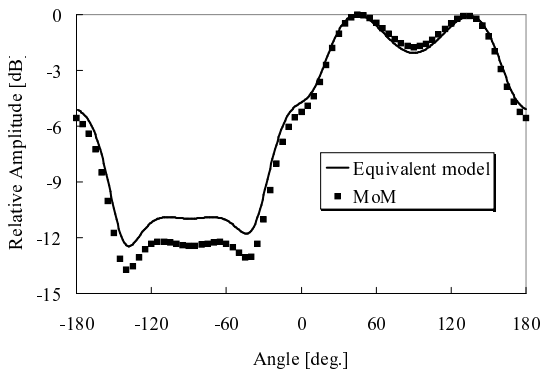

Fig. 2. Radiation patterns calculated by equivalent model and method of moment for the case of M = 5 and k = 1.

TABLE I
ANTENNA PARAMETER

Height H	λ/π
Line width L	$\lambda/80$
Array spacing G	$\lambda/4$
Gap D	$\lambda/200$
Number of ring elements M	1 – 8

the ports and enable the antenna to work even in the conformal configuration with large antenna length.

One wavelength ring element is assumed as a two-dipole array with a spacing of 0.27λ, and the antenna in Fig. 1 can be represented by an array of $2M$ equivalent dipole. This *equivalent model* makes it possible to formulate the antenna directivity in the ϕ plane as a function of reactances, as shown for the case of $M = 3$ and $k = 2$ in [10]. Here, the directivity function is generalized to the case of arbitrary values of M and k, as defined by a function of values of reactance circuits $\boldsymbol{x} = [x_1 \ \cdots \ x_{k-1} \ x_{k+1} \ \cdots \ x_{2M}]^T$ as follows:

$$D(\phi, \boldsymbol{x}) = \alpha \boldsymbol{w}(\boldsymbol{x})^T \boldsymbol{a}(\phi) \tag{1}$$

where α is a constant and the weight vector $\boldsymbol{w}(\boldsymbol{x})$ and steering vector $\boldsymbol{a}(\phi)$ are given by

$$\boldsymbol{w}(\boldsymbol{x}) = \left(Y^{-1} + X_r\right)^{-1} \boldsymbol{u}_k \tag{2}$$

$$\boldsymbol{a}(\phi) = \left[\exp\left\{j\frac{2\pi}{\lambda}\boldsymbol{r}_1^T \boldsymbol{L}(\phi)\right\} \cdots \exp\left\{j\frac{2\pi}{\lambda}\boldsymbol{r}_{2M}^T \boldsymbol{L}(\phi)\right\}\right]^T, \tag{3}$$

respectively, where

$$X_r = \mathrm{diag}\left[\ jx_1 \cdots jx_{k-1} \ z_s \ jx_{k+1} \cdots jx_{2M}\ \right] \tag{4}$$

$$\boldsymbol{u}_k = \left[\ \delta_{k-1} \ \cdots \ \delta_{k-2M}\ \right]^T \tag{5}$$

$$\boldsymbol{L}(\phi) = \left[\ \cos\phi \ \ \sin\phi \ \ 0\ \right]^T. \tag{6}$$

Here, $\boldsymbol{r}_i$ $(i = 1, \cdots, 2M)$ are the port positions of the equivalent dipoles, and Y is the mutual admittance matrix. δ_j is the Kronecker delta. Note that Y must be calculated in $2M$ full-wave simulations before using the directivity function (1). Practically, the variable reactance circuits are made of chip parts such as varactors, resistors, capacitors, and inductors, as described in [10].

To confirm the validity of the generalized directivity function, a pattern calculated by (1) was compared with a pattern calculated by the method of moment (MoM). Fig. 2 shows the result for the case of M = 5, k = 1, $\boldsymbol{x} = \left[\ 0 \cdots 0\ \right]^T$. The two patterns show good agreement, especially in the high-gain direction.

This formulation greatly reduces the complexity required to calculate directivity. More specifically, $\boldsymbol{x}$ is easier to obtain for a desired beamwidth in the practical stochastic simulations conducted in Section III-A. In addition, the derived steering vector (3) enables the implementation of the reactance-domain MUSIC algorithm described in Section III-B.

III. PERFORMANCE

In this Section, computer simulations are conducted to clarify the effect of the number of ring elements on the performance of beamwidth variation and DOA estimation based on the MUSIC algorithm. Below, a feed point is chosen as k = 1, so as to facilitate feed of the antenna. The other structural parameters of the calculated antenna are listed in Table I. The operating frequency is set to 2.4 GHz.

A. Beamwidth Control

MC simulations were conducted to obtain a set of $\hat{\boldsymbol{x}}$ that realizes a desired beamwidth ϕ_{h0} and a desired beam direction ϕ_0. The adopted metric here is given as follows:

$$\hat{\boldsymbol{x}} = \arg\max_{x}\{J\}, \tag{7}$$

where J is a proposed cost function to be maximized, which is defined as

$$J = (1-\beta)\, D(\phi_0, \boldsymbol{x})\,(1-\rho(\boldsymbol{x})) + \beta\left(1 - \frac{|\phi_h(\boldsymbol{x}) - \phi_{h0}|}{\phi_{h0}}\right). \tag{8}$$

$\phi_h(\boldsymbol{x})$ and $\rho(\boldsymbol{x})$ are the half-power beamwidth (HPBW) and reflection coefficient, respectively. In addition, $0 \le \beta \le 1$ is a simulation parameter to weight the first term with respect to the second term in (8). The first term represents the antenna

TABLE II
SIMULATION PARAMETERS

Weight β	0.5
Beam direction ϕ_0	0^o (fixed)
Beamwidth ϕ_{h0}	30^o – 150^o (every 5^o)
Number of ring elements	1 – 8
Variable range of $\boldsymbol{x}$	$-500\ \Omega < x_j < 500\ \Omega$

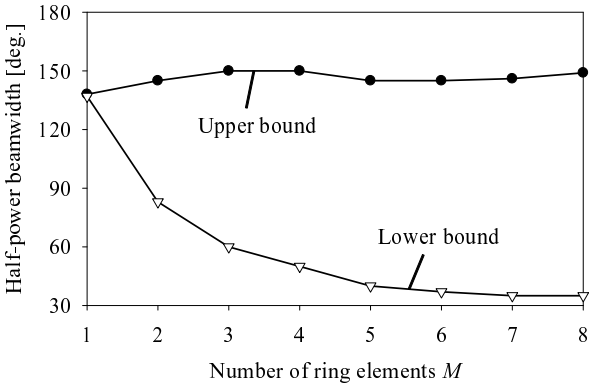

Fig. 3. Dependency of number of ring elements M on performance of beamwidth variation.

gain toward the desired beam direction, where the influence of impedance mismatch is taken into account. The second term represents the contribution of an incident beamwidth to the desired beamwidth.

Simulation parameters are listed in Table II. A total of 100,000 random sets of $\boldsymbol{x}$ were generated to obtain each solution for certain ϕ_{h0} and ϕ_0. The variable range of each component of $\boldsymbol{x}$ was given by $-500\ \Omega \leq x_j \leq 500\ \Omega$ ($j = 1, \cdots, k-1, k+1, \cdots, 2M$). In the present paper, we focus on the performance of beamwidth variation, as mentioned above. Thus, ϕ_0 was fixed to 0^o, and ϕ_{h0} was varied from 30^o to 150^o every 5^o. Note that $\boldsymbol{x}$, which gave $\rho(\boldsymbol{x}) > 0.5$, were eliminated from the results of the MC simulations so as to maintain the voltage standing-wave ratio (VSWR) below 3.0.

Fig. 3 shows the dependency of the number of ring elements M on the beamwidth-variation performance. Both the upper and lower bound of HPBW are indicated in the figure. It can be seen that the upper bound provides a nearly flat characteristic within the range of $1 \leq M \leq 8$. The upper beamwidth is mainly limited by the beamwidth of a single element (M = 1). On the other hand, the lower bound decreased with increase of M in the range of $1 \leq M \leq 5$. The effective antenna length could be extended to $M = 5$, by increasing the number of ring elements. For the case of $M = 5$, the antenna size was with $H \times W = 0.32\lambda \times 1.32\lambda$, and the upper and lower bound of HPBW were 145^o and 40^o, respectively. In the range of $M \geq 5$, the lower bound did not change significantly because the effective antenna length cannot be extended effectively. This is caused by the fact that it becomes difficult to retain the sufficient mutual couplings between the feed port and all of the other ports. In addition, the calculated dimension becomes higher with increase of M, which makes it difficult to obtain suboptimal solutions. In other words, higher computational complexity, i.e., the number of generated $\boldsymbol{x}$, is required in order to achieve a reasonable solution for cases in which the number of ring elements M is large. Next, Fig. 4 shows the calculated radiation patterns for case of $M = 5$. The reactance values obtained by MC simulation are listed in Table III. As the results indicate, the beamwidth effectively varied from 40^o to 145^o, while the main beam direction was approximately fixed to 0^o.

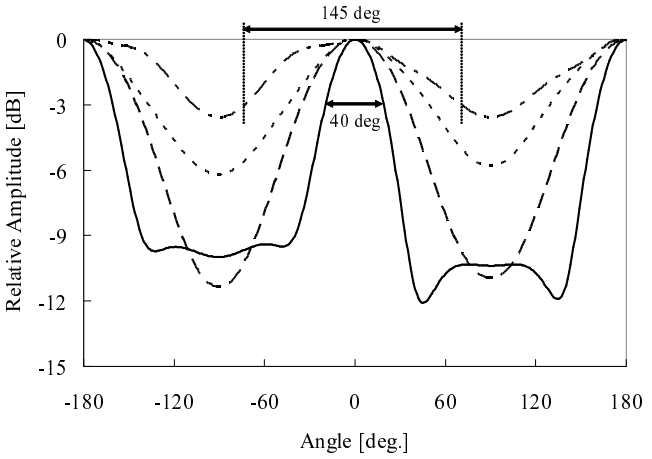

Fig. 4. Calculated radiation patterns of the proposed antenna with M = 5 and k = 1 in the E plane. (—-: ϕ_h=40^o, – –: ϕ_h=69^o, - - -: ϕ_h=93^o, – – –: ϕ_h=145^o.)

Note that it has been verified in [10] that the radiation patterns calculated by MoM agree to the experimental results in case of $M = 3$.

B. MUSIC

Reactance-domain MUSIC [11] was calculated in order to confirm that the number of estimated DOAs can be increased by increasing the number of ring elements M. Here, the algorithm is basically the same as that in [10].

The antenna with $M = 5$ was assumed, and the other antenna parameters were the same as those in Section III-A. Ten patterns are employed to implement MUSIC. The corresponding sets of reactance values are listed in Table IV. Each of the patterns is selected so that the beams have diverse directions. In the calculation, six uncorrelated waves with equal powers were generated, the DOAs of which were -170^o, -130^o, -60^o, 0^o, 55^o, and 125^o. The average received signal-to-noise ratio (SNR) of each of the waves was given by 20 dB. The number of DOAs was assumed to be known in advance.

Fig. 5 shows the results obtained by MUSIC with the total number of 10 $\times$ 1000 samples, and 10 $\times$ 100 samples. All six waves were estimated at high resolution in the case with 10 $\times$ 1000 samples. It can be also seen that, although the peaks become less sharp with the decrease of samples from 10 $\times$ 1000 to 10 $\times$ 100, the estimated DOAs remain precise. The theoretical maximum number of estimated DOAs was five for case of $M = 3$ [10]. Therefore, it was confirmed that the number of estimated DOAs can be increased with the increase in the number of ring elements.

TABLE III

INCIDENT VALUES OF REACTANCE CIRCUITS USED IN PATTERN SIMULATION.

	x_2	x_3	x_4	x_5	x_6	x_7	x_8	x_9	x_{10}
$\phi_h = 40^o$	487.1 Ω	101.2 Ω	484.1 Ω	187.3 Ω	172.8 Ω	364.3 Ω	166.1 Ω	447.8 Ω	-304.1 Ω
$\phi_h = 69^o$	495.5 Ω	27.7 Ω	407.6 Ω	399.6 Ω	451.0 Ω	-378.6 Ω	485.4 Ω	-38.5 Ω	-180.2 Ω
$\phi_h = 93^o$	466.2 Ω	448.3 Ω	425.5 Ω	-474.5 Ω	217.1 Ω	111.0 Ω	62.2 Ω	112.9 Ω	-410.7 Ω
$\phi_h = 145^o$	-441.1 Ω	-75.1 Ω	-355.7 Ω	-422.0 Ω	57.0 Ω	391.5 Ω	-391.8 Ω	-97.0 Ω	194.2 Ω

TABLE IV

INCIDENT VALUES OF REACTANCE CIRCUITS USED IN MUSIC SIMULATION.

	x_2	x_3	x_4	x_5	x_6	x_7	x_8	x_9	x_{10}
#1	412.2 Ω	350.4 Ω	-182.9 Ω	25.5 Ω	-434.9 Ω	130.4 Ω	142.5 Ω	-444.2 Ω	257.4 Ω
#2	-372.7 Ω	-142.3 Ω	-80.3 Ω	277.9 Ω	-469.9 Ω	173.1 Ω	-186.7 Ω	204.4 Ω	20.8 Ω
#3	-23.6 Ω	-141.4 Ω	494.0 Ω	-101.6 Ω	247.7 Ω	206.1 Ω	-31.5 Ω	-422.5 Ω	-112.2 Ω
#4	-297.5 Ω	89.1 Ω	-314.4 Ω	-57.3 Ω	53.7 Ω	-300.5 Ω	99.0 Ω	482.6 Ω	371.7 Ω
#5	-1.7 Ω	-281.1 Ω	-392.7 Ω	459.2 Ω	246.5 Ω	-14.2 Ω	144.6 Ω	321.6 Ω	418.5 Ω
#6	472.5 Ω	221.5 Ω	-374.0 Ω	-214.2 Ω	-231.5 Ω	100.5 Ω	391.5 Ω	287.9 Ω	348.4 Ω
#7	-375.6 Ω	-140.2 Ω	399.8 Ω	258.9 Ω	-216.6 Ω	218.8 Ω	272.6 Ω	-114.1 Ω	-210.0 Ω
#8	-23.8 Ω	-110.4 Ω	382.4 Ω	408.1 Ω	-97.9 Ω	-213.9 Ω	495.4 Ω	-82.1 Ω	355.1 Ω
#9	-208.0 Ω	93.0 Ω	263.6 Ω	-208.6 Ω	-2.4 Ω	409.8 Ω	-351.4 Ω	-9.4 Ω	-184.3 Ω
#10	138.8 Ω	-264.4 Ω	-67.4 Ω	129.4 Ω	-459.2 Ω	379.8 Ω	-192.7 Ω	-340.7 Ω	-74.0 Ω

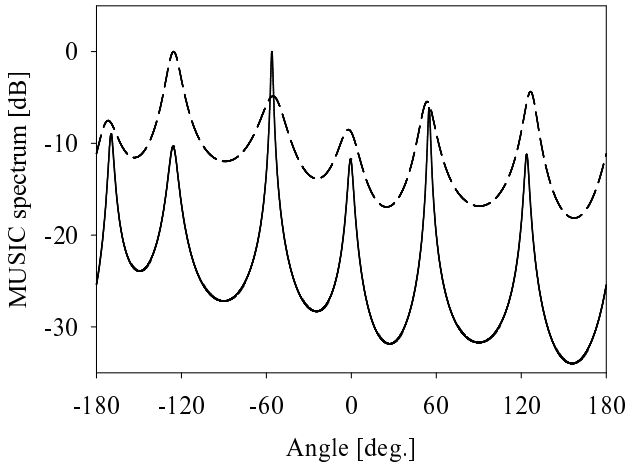

Fig. 5. Calculated MUSIC spectrum for 10×1000 samples (plain-line) and 10×100 samples (dashed-line), DOAs = -170^o, -130^o, -60^o, 0^o, 55^o, and 125^o. Average received SNR = 20 dB for each signal.

IV. CONCLUSION

An electronic beamwidth-control approach has been presented as an extension of a previously-proposed reactively-loaded ring antenna array. The antenna has a unique capability to increase the effective antenna length by increasing the number of ring elements. Computer simulations have clarified that the beamwidth-variation performance can be effectively improved by increasing M to five. In addition, the number of estimated DOAs based on the reactance-domain MUSIC algorithm was found to increase as well.

In order to solve a problem that this beamwidth-variable antenna radiates toward both sides, i.e., $\phi = 0^o$ and 180^o, the transparent artificial magnetic conductor (AMC) application described in [12] is a promising technique. The detailed investigation of the beamwidth-variable antenna combined with the transparent AMC is a subject for future study.

The proposed antenna will be useful for improving the performance of delay-restricted vehicle-to-vehicle communications without the requirement for a complicated cross-layer algorithm.

REFERENCES

[1] R. Ramanathan, J. Redi, C. Santivanez, D. Wiggins, and S. Polit, "Ad hoc networking with directional antennas: a complete system solution," *IEEE J. Select. Areas Commun.*, vol. 23, no. 3, pp. 496–506, Mar. 2005.

[2] K. Bhan, S. Ghosh, and G. Srivastava, "Study of control of beamwidth of radiation pattern of a waveguide using inclined slotted flanges," *IEEE Trans. Antennas Propag.*, vol. 26, no. 3, pp. 447–450, May 1978.

[3] A. Olver and J. Syed, "Variable beamwidth reflector antenna by feed defocusing," *IEE Proc. Microw., Antennas Propag.*, vol. 142, no. 5, Oct. 1995.

[4] P. Lampariello, F. Frezza, H. Shigesawa, M. Tsuji, and A. Oliner, "A versatile leaky-wave antenna based on stub-loaded rectangularwaveguide. I. Theory," *IEEE Trans. Antennas Propag.*, vol. 46, no. 7, pp. 1032–1041, July 1998.

[5] U. Sterr, A. Olver, and P. Clarricoats, "Variable beamwidth corner reflector antenna," *Electronics Letters*, vol. 34, no. 11, pp. 1050–1051, May 1998.

[6] S. Lim, C. Caloz, and T. Itoh, "Metamaterial-based electronically controlled transmission-line structure as a novel leaky-wave antenna with tunable radiation angle and beamwidth," *IEEE Trans. Microwave Theory Tech.*, vol. 53, no. 1, pp. 161–173, Jan. 2005.

[7] R. Harrington, "Reactively controlled directive arrays," *IEEE Trans. Antennas Propag.*, vol. 26, no. 3, pp. 390–395, May 1978.

[8] R. Dinger, "A planar version of a 4.0 GHz reactively steered adaptive array," *IEEE Trans. Antennas Propag.*, vol. 34, no. 3, pp. 427–431, Mar. 1986.

[9] C. Sun, A. Hirata, T. Ohira, and N. Karmakar, "Fast beamforming of electronically steerable parasitic array radiator antennas: theory and experiment," *IEEE Trans. Antennas Propag.*, vol. 52, no. 7, pp. 1819–1832, July 2004.

[10] S. Sugiura and H. Iizuka, "Reactively steered ring antenna array for automotive application," *IEEE Trans. Antennas Propag.*, vol. 55, no. 7, pp. 1902–1908, July 2007.

[11] C. Plapous, J. Cheng, E. Taillefer, A. Hirata, and T. Ohira, "Reactance domain MUSIC algorithm for electronically steerable parasitic array radiator," *IEEE Trans. Antennas Propag.*, vol. 52, no. 12, pp. 3257–3264, Dec. 2004.

[12] S. Sugiura and H. Iizuka, "Numerical study of steerable automotive antennas using artificial magnetic conductors," *IEEE AP-S Int. Symp. Dig.*, pp. 3352–3355, June 2007.